

Communication

Minimizing Voltage Ripple of a DC Microgrid via a Particle-Swarm-Optimization-Based Fuzzy Controller

Hussein Zolfaghari ¹, Hossein Karimi ², Amin Ramezani ³, Mohammadreza Davoodi ^{1,*}

¹ Department of Electrical and Computer Engineering, The University of Memphis, 3817 Central Ave, Memphis, TN 38111, USA; hzlfghri@memphis.edu

² Department of Electrical and Software Engineering, University of Calgary, Calgary, AB T2N 1N4, Canada; hossein.karimi@ucalgary.ca

³ Center for Innovation in Quality, Effectiveness and Safety, Baylor College of Medicine, Houston, TX 77021, USA; amin.ramezani@bcm.edu

* Correspondence: mdavoodi@memphis.edu

Abstract: DC microgrids play a crucial role in both industrial and residential applications. This study focuses on minimizing output voltage ripple in a DC microgrid, including power supply resources, a stochastic load, a ballast load, and a stabilizer. The solar cell serves as the power supply, and the stochastic load represents customer demand, whereas the ballast load includes a load to safeguard the boost circuits against the overvoltage in no-load periods. The stabilizer integrates components such as electrical vehicle batteries for energy storage and controlling long-time ripples, supercapacitors for controlling transient ripples, and an over-voltage discharge mechanism to prevent overcharging in the storage. To optimize the charging and discharging for batteries and supercapacitors, a multi-objective cost function is defined, consisting of two parts—one for ripple minimization and the other for reducing battery usage. The battery charge and discharge are considered in the objective function to limit its usage during transient periods, providing a mechanism to rely on the supercapacitor and protect the battery. Particle swarm optimization is employed to fine-tune the fuzzy membership function. Various operational scenarios are designed to showcase the DC microgrid's functionality under different conditions, including scenarios where production exceeds and falls below consumption. The study demonstrates the improved performance and efficiency achieved by integrating a PSO-based fuzzy controller to minimize voltage ripple in a DC microgrid and reduce battery wear. Results indicate a 42% enhancement in the integral of absolute error of battery current with our proposed PSO-based fuzzy controller compared to a conventional fuzzy controller and a 78% improvement compared to a PI controller. This translates to a respective reduction in battery activity by 42% and 78%.

Keywords: DC microgrid; fuzzy controller; particle swarm optimization; electric vehicles; voltage ripple minimization



Citation: Zolfaghari, H.; Karimi, H.; Ramezani, A.; Davoodi M. Minimizing Voltage Ripple of a DC Microgrid via a Particle-Swarm-Optimization-Based Fuzzy Controller. *Algorithms* **2024**, *17*, 140. <https://doi.org/10.3390/a17040140>

Academic Editor: Christos D. Zaroliagis

Received: 18 February 2024

Revised: 23 March 2024

Accepted: 26 March 2024

Published: 28 March 2024



Copyright: © 2024 by the authors. Licensee MDPI, Basel, Switzerland. This article is an open access article distributed under the terms and conditions of the Creative Commons Attribution (CC BY) license (<https://creativecommons.org/licenses/by/4.0/>).

1. Introduction

In the dynamic landscape of technology, microgrids play a crucial role in efficient energy management. DC microgrids, known for minimal losses and seamless integration with energy storage [1–3], are at the forefront. These systems, encompassing sources, control systems, loads, and energy storage, work collaboratively to mitigate the risk of power outages [4]. In [5], a method based on the battery state of charge (SOC) was employed to determine the power generated or consumed within a DC microgrid. The study incorporated battery management and switching control strategies to regulate the energy level of the DC microgrid. The authors of [6] emphasize the potential of DC microgrids to address challenges in coordinating distributed renewable energy, especially in mitigating adverse effects. However, integrating diverse power sources and storage presents chal-

allenges in voltage control and power-sharing, requiring effective control techniques, as highlighted in [4].

In the realm of microgrids, a key research focus lies in controlling and stabilizing their operation and performance. Dutta et al. [7] introduce a stabilizing controller for DC microgrids, employing a decentralized approach to enhance efficiency by considering various distributed energy resources (DERs) and energy storage elements such as EVs. Xia et al. [8] proposed a nonlinear decoupling method to address transient stability challenges in low-inertia DC microgrids. In [9], a bi-directional interlinking DC–AC converter utilized the AC frequency as a reference value for DC voltage and employed current feedforward control to align the DC voltage with the AC frequency, enhancing stability and controllability in low-inertia DC microgrid systems. The study by [10] focuses on the design and analysis of controlling and optimizing the operation of a DC microgrid with DERs such as photovoltaic (PV). It examines efficiency improvements through a bi-directional DC/DC converter, contrasts various maximum power point tracking (MPPT) techniques, and reports the results of stability analysis using the Lyapunov function, discussing a variety of controllers including fuzzy, MPC, and Robust [11]. Recent studies have increasingly focused on fuzzy logic, PSO, and their combination [12–14]. The study explains how DERs like diesel engines, micro turbines, fuel cells, photovoltaics (PVs), and small wind turbines are utilized in microgrids. Effectively managing microgrids involves controlling and operating these DERs along with adjustable loads and storage devices such as flywheels, energy capacitors, and batteries. This coordination is crucial for the overall functioning of a microgrid.

Leveraging DERs like PV technology presents a viable and economically efficient solution to mitigate pollution and warming, especially in microgrid applications [15,16]. Authors in [17–19] emphasize the significance of these energy sources for microgrid applications. The authors of [20] highlight the potential superiority of photovoltaic-based DC microgrids over traditional AC grids. Due to the unpredictable nature of renewable resources, effective storage solutions like batteries and energy storage systems play a crucial role in enhancing microgrid efficiency [21,22]. Additionally, [23] emphasizes the significance of energy storage systems, especially EVs, in distributed systems to conserve energy and address the unpredictability of renewable energy sources, while integrating EVs into microgrids is proposed to strengthen energy storage, concerns about battery lifespan exist [24]. Ref. [25] presented a technique, called Integrated Battery Life Loss Modeling and Anti-Aging Energy Management (IBLEM), to handle battery aging in battery energy storage systems (BESSs) like EV batteries. The authors of [26] proposed a PV-embedded series DC electric spring (PVES) to reduce battery storage in DC microgrids with significant PVs. IBLEM quantifies aging costs and optimizes energy management strategies to tackle challenges and support the advancement of transportation electrification. Given the unpredictable nature of DERs (especially photovoltaic sources), nondeterministic load, and energy storage (e.g., EVs), DC microgrids incorporating these energy production units are prone to experiencing ripples. The imperative approach in such systems is the crucial task of minimizing these ripples, as emphasized by Fazal et al. [27].

The integration of renewable energy sources in microgrids introduces ripples, posing challenges to power quality (PQ), which is crucial for energy efficiency and equipment operation [28,29]. Various methods for ripple minimization exist. Chaturvedi et al. [30] propose an adaptive voltage-tuning-based load-sharing strategy for DC microgrid ripple minimization. Ferahtia et al. [31] introduce an adaptive droop-based control strategy to efficiently minimize ripples. Sekhar et al. [32] investigate voltage control strategies, emphasizing the impact of voltage control devices on distribution system ripples. Addressing voltage stabilization and ripple minimization challenges, refs. [33,34] highlights the role of microgrid components, including energy storage, in stabilizing bus voltage during black-outs and minimizing ripples under challenging grounding conditions, while certain studies address ripple minimization in DC microgrids with energy storage systems like EVs and DERs such as PVs [35,36], there is untapped potential for investigating fuzzy optimization controllers to minimize ripples and improve power quality in the DC microgrids.

This research aims to simulate a DC microgrid comprising stochastic renewable energy resources (e.g., PV), stochastic load, ballast load, and a stabilizer. The fuzzy controller regulates the switching rate of stabilizer components, enabling efficient control of the system. This work improves the fuzzy controllers in microgrids [35,36] by training the fuzzy membership functions using PSO. This training improves the performance of the traditional fuzzy controller by considering the goals defined in the objective function. Additionally, unlike other papers that used EV batteries as energy storage in DC microgrids [37], this study considers the battery charge and discharge to lower its wear and tear. This consideration plays a crucial role in increasing battery lifetime, addressing a limitation overlooked in prior research involving EV batteries.

2. Problem Formulation

The study is dedicated to minimizing ripples and extending the lifespan of EV batteries. Achieving these objectives involves simulating a system with four essential components: the power source, stochastic load, ballast load, and stabilizer. Figure 1 visually represents the microgrid structure. In this paper, we introduce an optimized controller based on the PSO algorithm to overcome the limitations of previous research in reducing battery activity frequency. This represents a significant advantage of using the PSO algorithm in our study. The main difference lies in optimizing the rules of the fuzzy controller to minimize the number of battery activities and reduce voltage ripples. Subsequent sections will clarify detailed explanations of each part of this DC microgrid, outlining the diverse components within each.

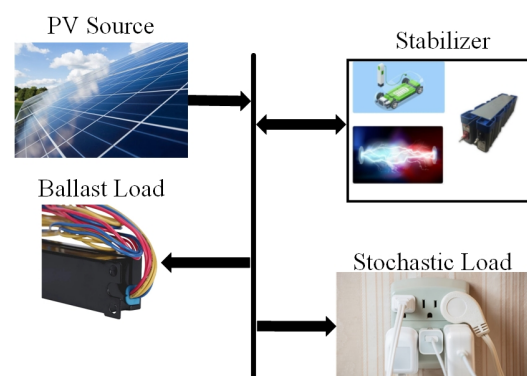


Figure 1. Simplified microgrid model [35,38].

2.1. Model of Stochastic Power Source

The efficient operation of each solar system necessitates maximum power point tracking (MPPT). This paper assumes that the maximum power points of a photovoltaic system have been monitored. The DC microgrid receives its power from the photovoltaic system's maximum power output, which is a random number. The term "random" is employed due to the unpredictable nature of weather and the inherently random power generation by solar cells. The power generated may vary, sometimes falling short of consumption and occasionally exceeding it. To simulate variability and randomness, a pseudo-random number generator is employed to supply power, and simultaneously, a boost converter tracks these changes, generating the output power of these PVs. The duty cycle of the transistor in the structure of the boost converter, shown in Figure 2, is set by a random number matched with the maximum output power of PVs. This ensures that the boost converter can follow the maximum power points generated by the PV system.

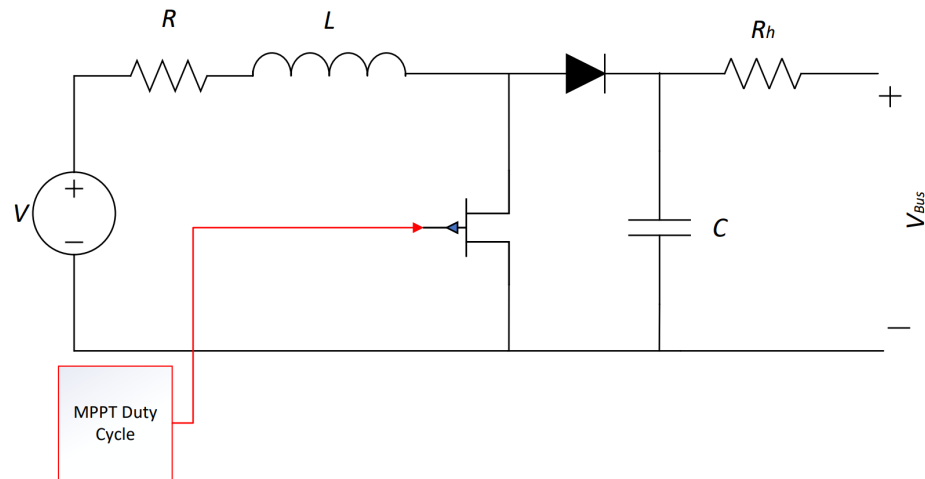


Figure 2. Power source model, where R is the boost converter resistor, L is the boost converter inductance, C is the DC link capacitor, R_h is the connection resistor, and V_{Bus} is the DC microgrid bus voltage [35].

2.2. Model of Stochastic Load

The load model includes a buck converter that demonstrates the customer’s usage pattern by dissipating power. The stochastic load model is illustrated in Figure 3. At the coupling point between the load and the DC microgrid, there is a capacitor that charges from the main bus. Once it is fully charged, it discharges into the buck converter, which serves to model the load of the system.

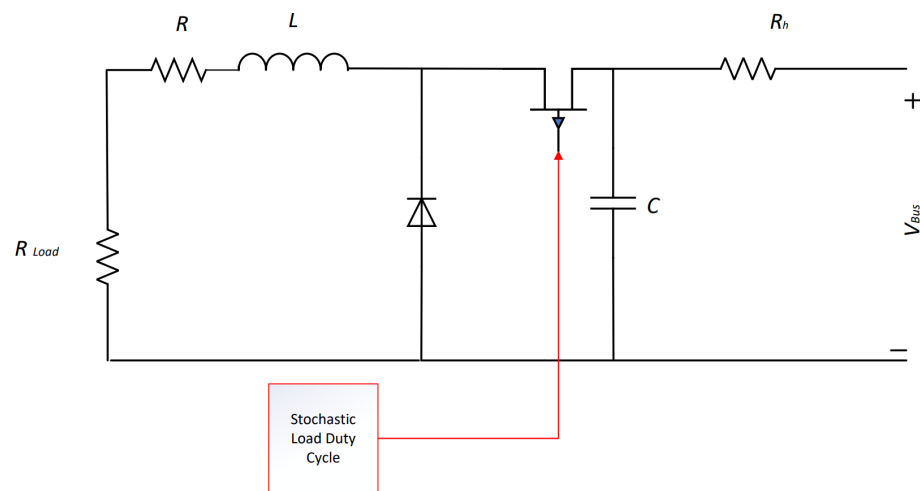


Figure 3. Load model, where R_{Load} is the stochastic load model, R is the buck converter resistor, L is the buck converter inductance, C is the DC link capacitor, R_h is the connection resistor, and V_{Bus} is the DC microgrid bus voltage [35].

2.3. Stabilizer Model

The DC microgrid’s stabilizer model includes three main parts: the EV battery, supercapacitor, and over-voltage discharge. An EV battery and a supercapacitor are connected to the DC microgrid through a buck–boost converter. The boost converter is active during charging, and the buck converter is active during discharging. However, the role of the overvoltage discharge unit, which only has a buck converter, is to waste excess voltage. The over voltage discharge (OVD) unit engages when batteries and supercapacitors are fully charged, preventing overcharging. It is linked to a buck converter, managing surplus PV generation by dissipating extra voltage. Each stabilizer converter has one transistor,

controlled by a controller discussed in the following section. The stabilizer unit structure is demonstrated in Figure 4.

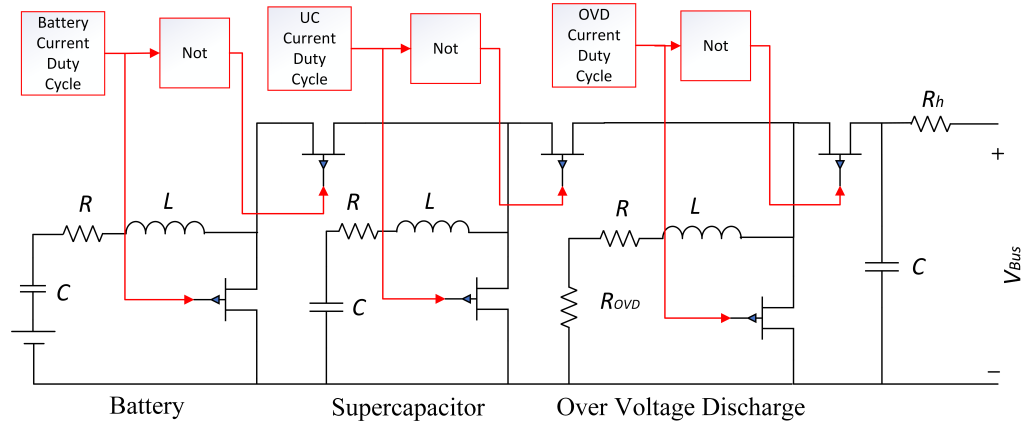


Figure 4. Stabilizer model, where R is the buck–boost converter resistor, L is the buck–boost converter inductance, C is the DC link capacitor, R_h is the connection resistor, and V_{Bus} is the DC microgrid bus voltage [35].

2.4. Ballast Load

Given the presence of boost converters in the grid, ensuring a minimal load on the DC microgrid is essential at all times. An unloaded boost converter can cause voltage spikes, leading to instability and potential damage. Hence, a large-value resistor is incorporated into the grid as a ballast load to safeguard the DC microgrid circuits.

3. Methodology

This paper has two primary objectives: reducing output voltage ripple and minimizing the charging and discharging cycles of EV batteries. To achieve these goals, an objective function is utilized. The first part of this function focuses on minimizing the square value of the ripple, guiding the controller to generate signals that activate the EV battery and supercapacitor, assisting the source of the DC microgrid in tracking the reference output bus voltage. The primary controller is a fuzzy controller, discussed in the next subsection. The second objective aims to minimize the number of charge and discharge cycles of the EV battery to extend its lifespan, as the lifespan is directly related to these cycles. The second part of the objective function reduces the square sum of the EV battery current, thus minimizing the charging and discharging cycles. This objective is achieved by activating the supercapacitor to handle short-time ripples and engaging the battery only in cases of longer-time ripples in the output voltage. Consequently, the objective function is defined as follows:

$$OF = \int_0^\tau (v_{Ripple})^2 dt + 0.1 \int_0^\tau I_{battery}^2 dt \tag{1}$$

$$v_{Ripple} = v_{bus} - 100 \tag{2}$$

v_{bus} : The voltage of DC microgrid bus voltage;

$I_{battery}$: The battery current;

v_{Ripple} : The difference between bus voltage and reference voltage.

The optimization and adjustment of the controller to meet these goals will be explained in the following subsections.

3.1. Control Design

Our proposed controller in this work is a fine-tuned version of the fuzzy controller using particle swarm optimization (PSO). More specifically, our approach merges fuzzy logic and PSO, optimizing both the expectation and standard deviation of the fuzzy controller’s membership functions. The fuzzy controller incorporates four inputs: bus voltage error, integral of bus voltage error, battery state of charge (SoC), and supercapacitor state of charge (SoC). From these inputs, the fuzzy controller generates current references for the battery, supercapacitor, and overvoltage discharge (OVD). Three low-level PI controllers process reference values and generate duty cycles for stabilizer components based on actual component currents.

The controller generates the duty cycle to change the switching rates of the EV’s battery, supercapacitor, and OVD in the following manner.

- Duty cycle signals initiate battery or supercapacitor discharge into the DC microgrid when production is lower than consumption, providing additional electrical energy.
- When the battery and supercapacitor are fully charged and the production exceeds consumption, these signals discharge overvoltage on the OVD component to prevent overcharging, ensuring safety.
- Alternatively, these duty cycles can be applied to the boost converters of the battery or supercapacitor to charge them when their charge is below the full amount.

Figure 5 illustrates the overall architecture of the proposed fuzzy controller.

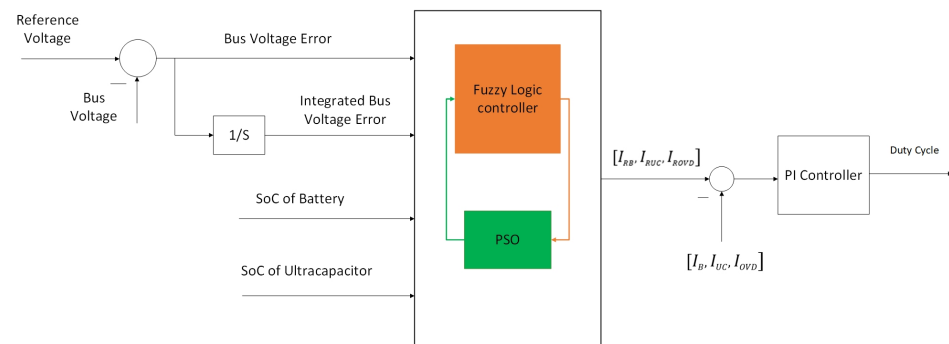


Figure 5. Configuration of fuzzy controller, where I_B is battery current, I_{UC} is supercapacitor current, I_{OVD} is OVD current, I_{RB} is battery reference current, and I_{RUC} is supercapacitor reference current.

Similar to [35,36], the primary fuzzy controller’s membership functions are initially untrained. However, in the trained version, they undergo fine-tuning via PSO to achieve the objectives of ripple minimization and battery lifetime expansion. Figure 6 shows the membership function of the bus voltage error and the membership function of the integrated bus voltage error. Two membership functions, negative (NEG) and positive (POS), are considered for each input. The NEG is designed to manage negative voltage ripple, whereas the POS is employed to address positive voltage ripple. It is worth mentioning that the currents and voltages are normalized before feeding into the fuzzy inference system. The fuzzy controller functions effectively by taking two parameters as inputs: the integral of voltage error and the voltage error itself. This enables the algorithm to discern alterations that could influence the bus voltage, aiding in the preservation of the nominal voltage level. The input associated with the voltage error promptly reacts to rapid fluctuations, whereas the integral term identifies prolonged changes. Consequently, the fuzzy controller initiates responses to counteract and rectify any deviations in the bus voltage. This dual-response mechanism empowers the DC microgrid to address both swift and gradual alterations, thereby widening its bandwidth and enhancing its ability to promptly adapt to varying conditions.

Moreover, Figure 7 shows the membership functions associated with the state of charge (SOC) of the battery and supercapacitor, respectively. The SOC of the battery and

ultracapacitor are treated differently since they have two distinct objectives: “low” and “high”. Although it may seem that these functions do not cover certain sections of the axis, it is essential to note that the “NOT” operation of each membership function is considered in the rule base so it can cover the entire range between 0 and 1.

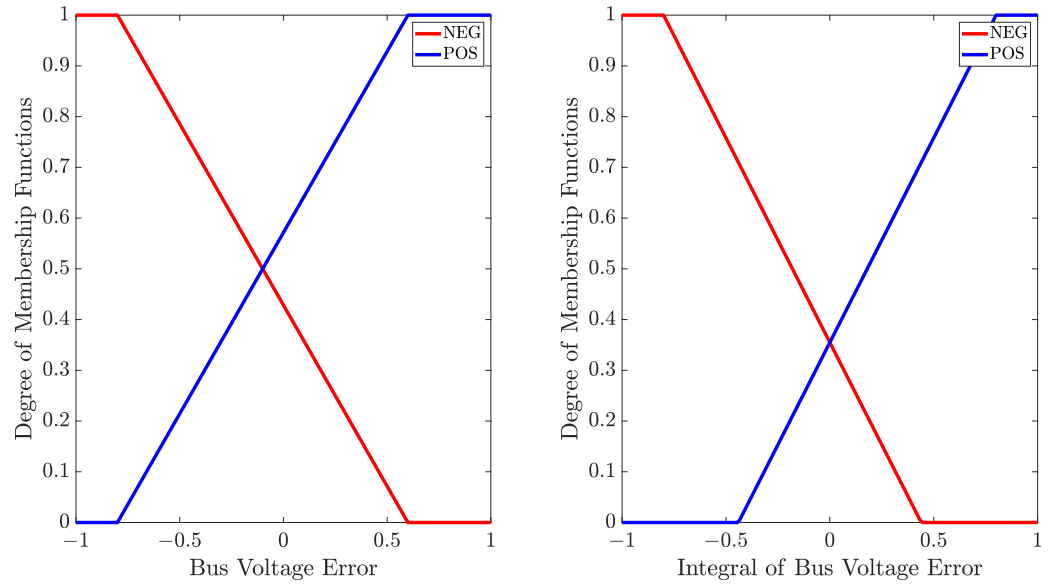


Figure 6. The membership function for the bus voltage error and its integral [35].

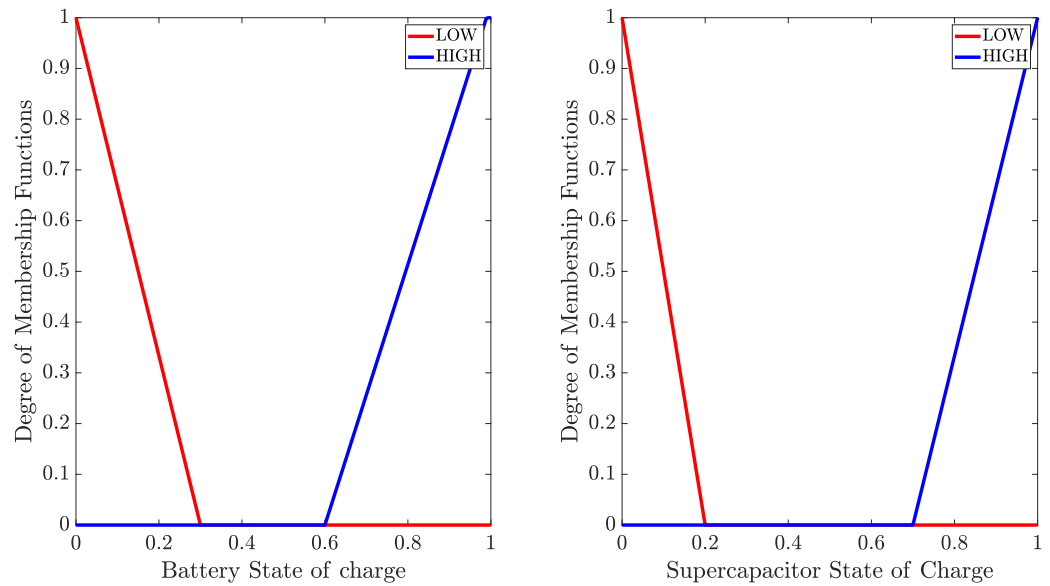


Figure 7. The membership functions for state of charge of battery and supercapacitor [35].

To minimize the usage of the EV battery, a low charge condition is defined as 0.3, while a high charge condition is set to 0.7. These conditions are strategically established to reduce the overall engagement of the EV battery. Figure 7 clearly illustrates the distinction between high and low battery charge levels. Furthermore, the boundaries for the supercapacitor, Figure 7, are extended to ensure its activation during nearly all short-time ripples. This deliberate extension is designed to prevent the EV battery from being active during such ripples, ultimately contributing to the extension of the EV battery’s lifespan.

Figure 8 illustrates the membership functions representing the reference currents for the battery, ultracapacitor, and over voltage discharge (OVD). The current is normalized and constrained between -1 and 1 . A positive value indicates that the current is injected into the grid (energy storage discharges into the DC microgrid), while a negative value

represents the opposite. The battery’s output current is characterized by five Gaussian membership functions, while the ultracapacitor features four membership functions. It is noteworthy that a zero-membership function is specified for the EV battery, reflecting its heightened sensitivity to activation.

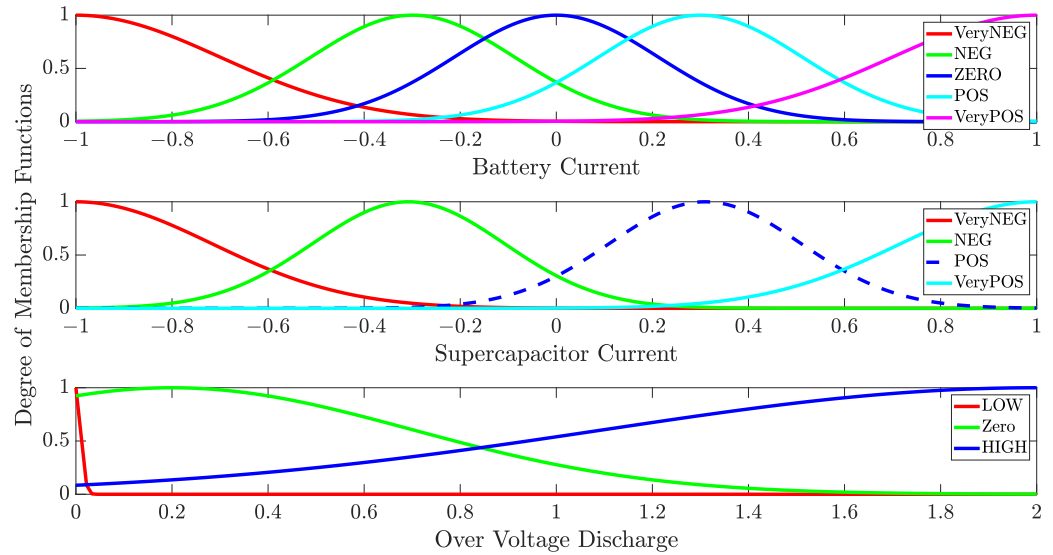


Figure 8. Membership functions for the EV’s battery, ultracapacitor, and OVD.

Fuzzy Rules

The input and output specifications for the fuzzy inference system are listed in Table 1. It is noteworthy that the voltage error in Table 1 is defined as follows:

$$\text{Voltage Error} = V_{\text{nominal}} - V_{\text{MG}}, \tag{3}$$

where V_{nominal} denotes the reference voltage level in the microgrid, and V_{MG} denotes the actual measured voltage. In this equation, when the voltage of the DC microgrid exceeds the reference voltage, the error is negative; conversely, when the DC microgrid falls below the reference voltage, the error is positive. This distinction is pivotal in delineating the operational state of the microgrid and will inform the formulation of fuzzy rules.

Table 1. Input and outputs of the fuzzy interface system.

Input and Output	Term
Bus voltage error	e
Integrated bus voltage error	$\int e dt$
Battery voltage	v_b
Ultracapacitor voltage	v_u
Battery current	i_b
Ultracapacitor current	i_u
Over-voltage discharge current	i_o

A total of 20 rules have been defined to map the inputs to the outputs, as shown in Table 2. Rules 1 through 6 establish relationships between the battery voltage and the bus voltage. For instance, Rule 1 indicates that when v_b is “not high”, v_u is “high”, and both e and $\int e dt$ are “negative”, then i_b should be “very neg”, suggesting that the bus voltage is higher than the nominal value and the battery is not fully charged, allowing it to store excess energy. Rules 7 to 10 define the relationships between the ultracapacitor and the bus voltage. Rules 11 to 16 represent the overvoltage discharge (OVD) phase, and rules 17 to 20 determine the energy transfer between the battery and the ultracapacitor.

Table 2. Rules of the fuzzy controller.

Rules	v_b	v_u	e	$\int e dt$	Then	i_b	i_u	i_o
1	Not high	High	Negative	Negative	then	Very Neg	-	-
2	Not high	Not low	Negative	-	then	Neg	-	-
3	Not low	Not high	Positive	-	then	Pos	-	-
4	Not low	Low	Positive	Positive	then	Very Pos	-	-
5	-	Not Low	Positive	-	then	Zero	-	-
6	-	Not high	Negative	-	then	Zero	-	-
7	-	Not high	Negative	Negative	then	-	Very Neg	-
8	-	Not high	Negative	-	then	-	Neg	-
9	-	Not low	Positive	-	then	-	Pos	-
10	-	Not low	Positive	-	then	-	Very Pos	-
11	High	High	Negative	-	then	-	-	Low
12	High	High	Negative	Negative	then	-	-	High
13	Not high	-	-	-	then	-	-	Off
14	-	Not high	-	-	then	-	-	Off
15	-	-	Not Pos	-	then	-	-	Off
16	-	-	-	Not Pos	then	-	-	Off
17	High	Low	-	-	then	Pos	-	-
18	High	Low	-	-	then	-	Neg	-
19	Low	High	-	-	then	Neg	-	-
20	Low	High	-	-	then	-	Pos	-

3.2. Optimization Method

The optimization method employed in this study is the particle swarm optimization (PSO) algorithm [39,40], a widely recognized metaheuristic algorithm known for its rapid convergence. In this research, the PSO algorithm seeks the optimal values for the expectations and standard deviation of Gaussian membership functions to determine the best references for the current of the battery, supercapacitor, and OVD components. The algorithm operates by searching for optimal values that minimize the objective function. This function, as explained earlier in (1), comprises two components: one for ripple minimization and another for reducing the number of EV battery activations. The proposed PSO-based fuzzy controller is implemented based on the Algorithm 1.

Algorithm 1 Algorithm of the PSO-based fuzzy controller:

1. Determine the PSO parameters.
 2. Define boundaries for the expectation and standard deviation of each membership function.
 3. Initialize the fuzzy inference system (FIS).
 4. PSO updates the positions and velocities of each population.
 5. PSO executes DC microgrid model and provides it with a new FIS. After simulation, PSO calculates the objective function value.
 6. If the results from this new FIS can minimize the cost function more effectively than the results from other populations, it should be saved as the best solution among all population results.
 7. If the stop condition is not met, go to step 4.
 8. Print the results.
-

4. Simulation Results

In this section, we present simulation results of our proposed PSO-based fuzzy controller on a DC microgrid, comparing it with two conventional controllers to demonstrate its efficiency.

4.1. Initialization and Fuzzy Optimization

To start simulating the DC microgrid, we require the values of the parameters of this system. Initially, a model of the DC microgrid is implemented in MATLAB/Simulink 2022, and the associated parameters are as follows:

$$\begin{aligned}
 C &= 20 \times 10^{-6} \quad (\text{Used in ballast}) \\
 R &= 50 \quad (\text{Used in ballast}) \\
 L &= 0.001 \\
 R_{Bi} &= 0.2 \quad (\text{Battery resistor}) \\
 L_B &= 0.0011 \quad (\text{Inductance for battery converter}) \\
 R_{Bb} &= \frac{0.4}{4} \quad (\text{Resistor of inductance for battery converter}) \\
 V_{BBase} &= 47.2 \quad (\text{Battery base voltage}) \\
 C_B &= 3000 \quad (\text{Capacitor capacity for the battery}) \\
 C_C &= 150 \quad (\text{Ultra capacitor (UC) capacity}) \\
 L_C &= 0.0011 \quad (\text{Inductance of converter of UC}) \\
 R_{CL} &= 0.4 \quad (\text{Resistor of converter of UC}) \\
 R_O &= 5.6 \quad (\text{OVD resistor as a load}) \\
 R_{OL} &= 2 \quad (\text{OVD resistor of converter}) \\
 L_O &= 0.0006 \quad (\text{Inductance of converter of OVD}) \\
 R_{HI} &= 0.2 \quad (\text{Output resistor of stabilizer}) \\
 C_M &= 0.001018 \quad (\text{Stabilizer output capacity}) \\
 R_{High} &= 0.2 \quad (\text{Stabilizer output resistor}) \\
 R_{Low} &= 0.2
 \end{aligned}$$

To design the PSO-based fuzzy controller, we utilized the PSO algorithm to optimize the parameters of the fuzzy controller. The convergence diagram of the PSO algorithm is plotted in Figure 9 to illustrate how effective the algorithm is at optimizing fuzzy controller parameters. To provide a comparison between the fuzzy membership functions before and after optimization through PSO algorithm, these results are shown in Figures 8 and 10.

We conducted testing and evaluation on three different types of controllers, namely PI (implemented according to [35]), fuzzy, and PSO-based fuzzy controllers. To compare the results of our proposed controller, the PSO-based fuzzy controller, with the other two controllers, we require a load and power benchmark. The information regarding the load and source power used in our system is provided in Figure 11. In the subsequent sections, we compare the results of our proposed controller in this paper with the other two controllers.

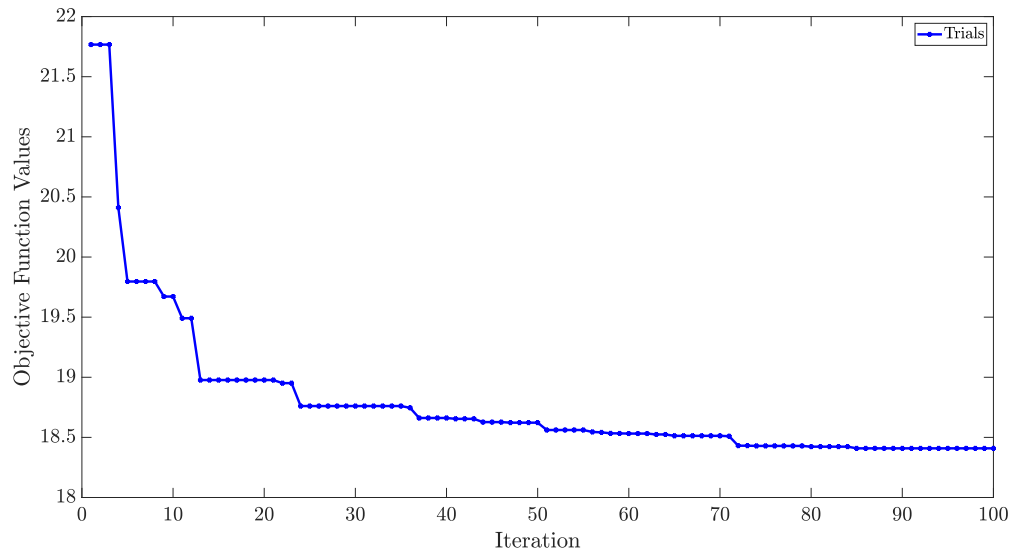


Figure 9. Convergence of objective function.

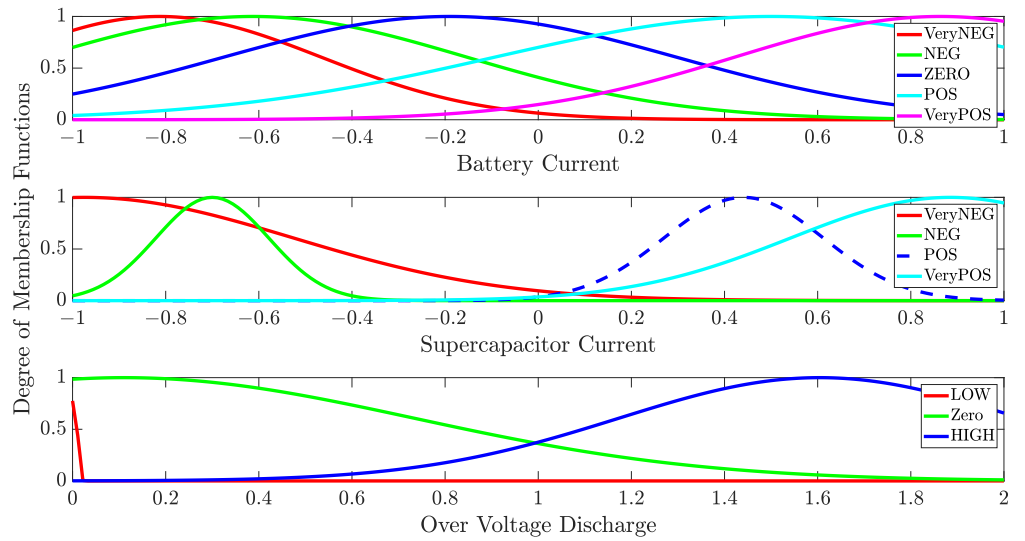


Figure 10. Membership functions for the EV's battery, ultracapacitor, and OVD after optimization.

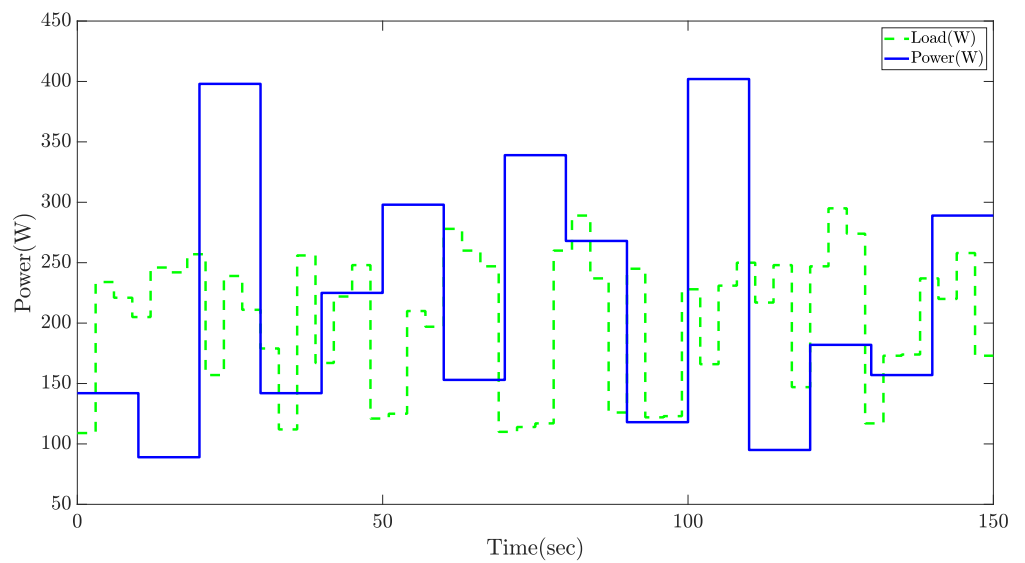


Figure 11. The value for load consumption and resource production.

4.2. Ripple Minimization

One of the main objectives of this research is to minimize the voltage ripple in the main bus. In this section, we will explain this objective further to demonstrate the effectiveness of our proposed controller compared to the two other controllers. The voltage ripples of the system in the presence of three introduced controllers are shown in Figure 12. As can be seen from this figure, the regular fuzzy controller is the most inefficient in ripple minimization. By comparing the performance of the two other controllers with the dashed black line, which represents a 100-volt reference, it becomes apparent that our proposed controller performs better. Furthermore, we will report the integral of absolute error for these three methods in Table 3 to quantitatively compare their effectiveness in minimizing voltage ripples.

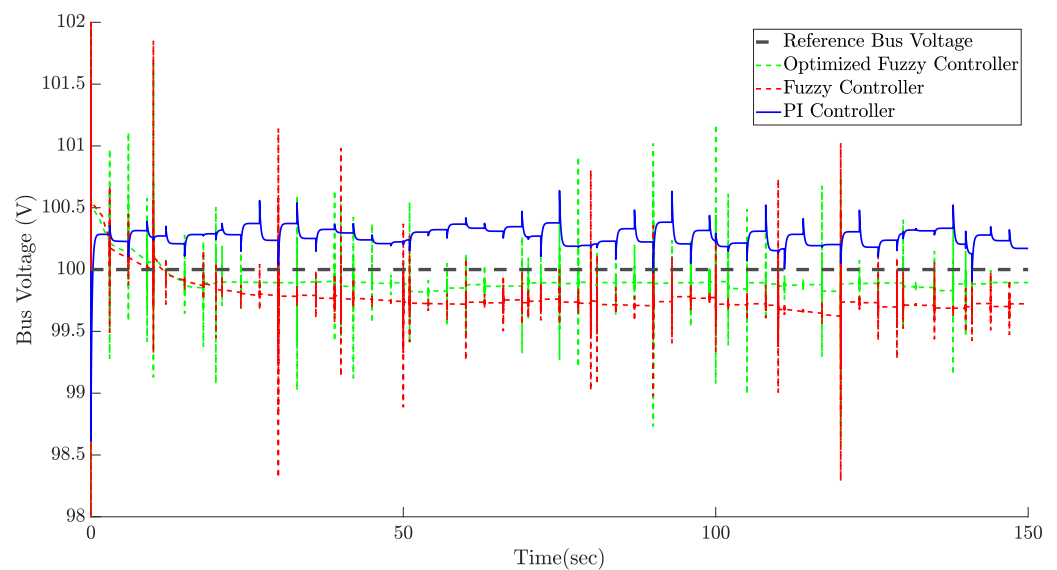


Figure 12. The output voltage of the DC microgrid: a comparison for all scenarios.

Table 3. Integral of absolute error (IAE) for voltage ripple of the DC microgrid bus.

Methods	IAE
PI controller	33.5499
Fuzzy controller	37.3996
PSO-based fuzzy controller	18.768

4.3. Battery Current Minimization

Our proposed controller aims to optimize the utilization of the EV battery by reducing its activity. This approach leverages the supercapacitor's shorter charging and discharging times, allowing it to compensate for most short-term changes in system load and voltage ripples. As a result, the system bandwidth is significantly enhanced due to the fast responses to the effects of load and source changes on the bus voltage of the DC microgrid. Moreover, this strategy reduces the wear and tear on the battery from frequent use compared to the supercapacitor. The supercapacitor is also more cost-effective and easier to replace within the system than the EV battery. The flow of current for the battery, supercapacitor, and stabilizer are important, and have been shown in Figure 13. In this figure, by comparing the middle figure with the bottom one, we can determine when the battery, supercapacitor, or both are charging and when they are discharging. To illustrate how the system achieves this process, it is important to consider the total value of the battery current during operation, as shown in Figure 14. Although it may not be evident in the Figure 14, when employing the PSO-based fuzzy controller, the current drawn by the battery is substantially lower than the total value of the two other controllers, as shown in

Table 4. This reduction in current drawn by the battery demonstrates the effectiveness of our approach.

Table 4. Integral of absolute error (IAE) for the battery current.

Methods	IAE
PI controller	304.5562
Fuzzy controller	118.5752
PSO-based fuzzy controller	67.1039

As shown in Figure 15, the value of the supercapacitor current increases due to its operation in attenuating most of the ripples in the DC microgrid. To determine which controller performs better, it is essential to consider both Figures 14 and 15. This comparison helps identify which controller contributes more to reducing the battery current while also minimizing ripple in the DC microgrid bus voltage.

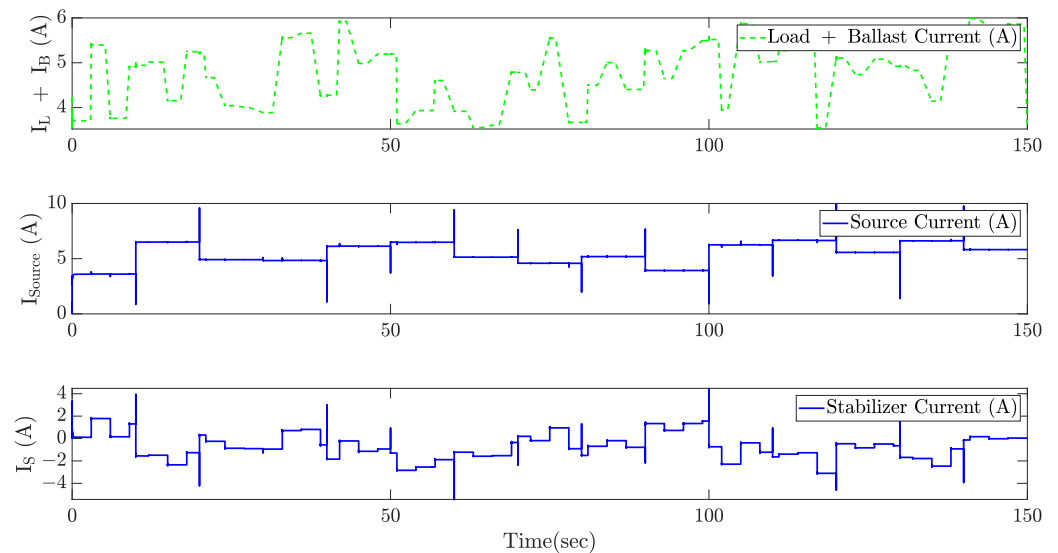


Figure 13. The current of power source, load, and stabilizer.

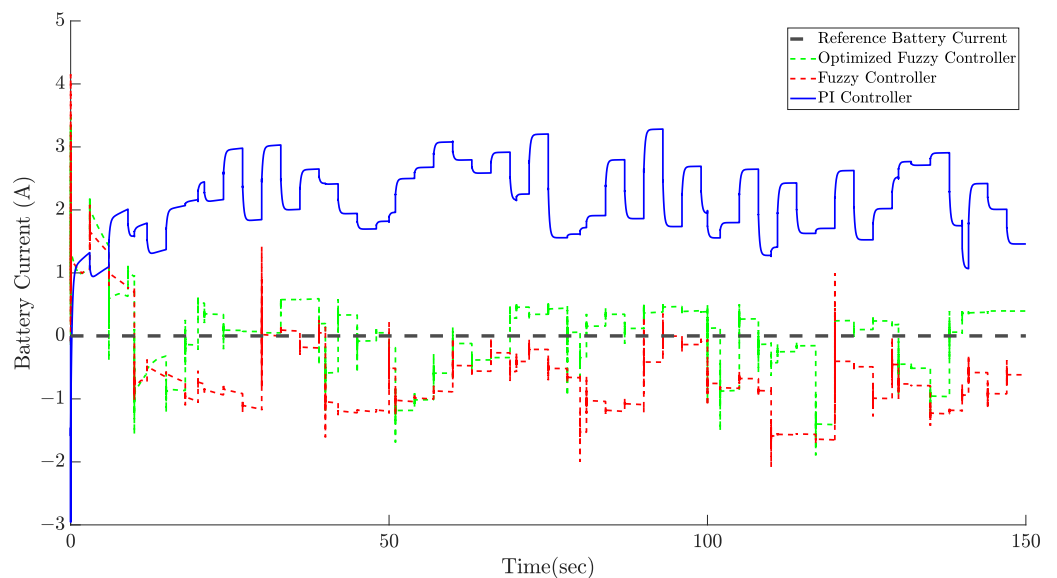


Figure 14. The current of battery in three scenarios.

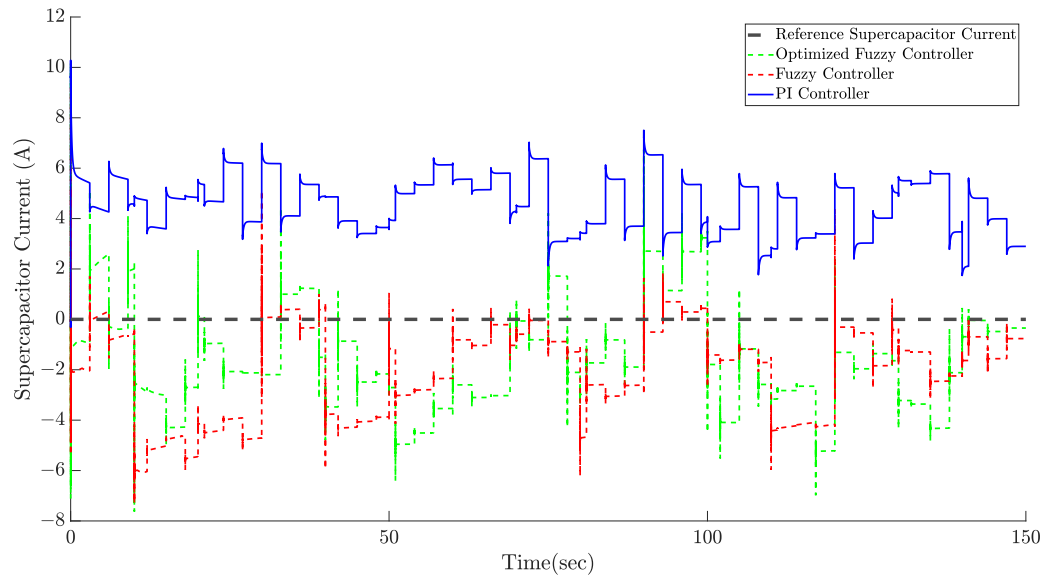


Figure 15. The current of the ultracapacitor in three scenarios.

4.4. Energy Transfer between Battery and Supercapacitor

Another innovative aspect explored in this study is the ability to transfer energy between the battery and supercapacitor, as illustrated in Figure 16. This capability is highlighted due to the rapid charge and discharge times of the supercapacitor compared to the battery. There are two notable advantages to this energy transfer between the two components. Firstly, it helps prevent battery damage by avoiding discharge below the undercharge level. Secondly, it reduces the frequency of battery usage for ripple minimization. These advantages will be further elucidated in the subsequent discussion. Even if in Figure 16 there is a small difference between two scenarios, this small variation helped the system to reduce the battery current drawn because of charge and discharge.

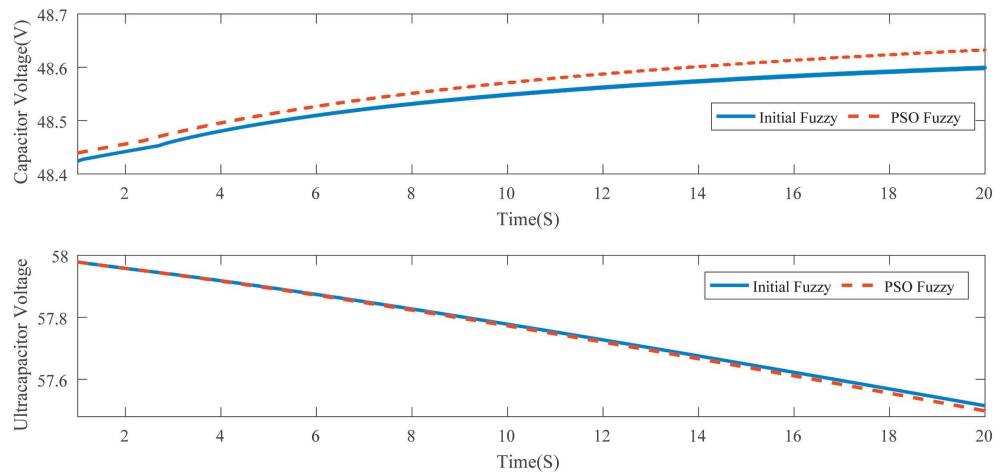


Figure 16. Energy transfer between battery and supercapacitor.

The rapid energy transfer between critical components is demonstrated in Figure 16, facilitating swift recharge and reducing the risk of undercharging and damage, especially to the battery. Notably, this process does not significantly alter the charge level of the components. Conversely, when the battery is fully charged and the supercapacitor is depleted, energy redirection occurs, effectively reducing system ripples through supercapacitor operation and lowering battery activation frequency; while immediate outcomes may not be evident, a comparison of total current drawn from the battery across controllers highlights the approach’s efficacy in achieving objectives.

5. Conclusions

This paper has introduced a novel method for controlling DC microgrids utilizing a fuzzy controller with four input variables: bus voltage error, integrated error of bus voltage, state of charge (SOC) of the battery, and SOC of the ultracapacitor. The fuzzy controller generates three current references for the EV battery, supercapacitor, and OVD. These references are compared with the actual values of the currents of these three components. The resulting values are fed as inputs to a PI controller, which produces the duty cycle to control the switching rate of these components. The switching and energy exchange between the stabilizer, power source, and load collaboratively reduce the ripples in the output voltage and minimize the battery activation frequency to enhance the battery's lifespan. Simulation results affirm the successful minimization of bus voltage ripple through this method. The optimized signals in the output of the fuzzy controller for the three elements of the stabilizer fulfill both objectives. To summarize, the core findings of this paper are as follows:

1. Development of a new PSO-based fuzzy controller designed to minimize the ripple of DC microgrid bus voltage and reduce battery activation frequency.
2. Implementation of energy transfer between the supercapacitor and the battery to minimize ripple and increase battery lifespan.

Future work will explore other types of energy resources, such as wind and fuel cells, and provide conditions for droop control. Additionally, implementing state space equations and integrating a linear quadratic tracker to track the reference voltage are noteworthy avenues for further exploration.

Author Contributions: Conceptualization, H.Z., A.R. and M.D.; methodology, H.Z. and H.K.; software, H.Z. and H.K.; writing—original draft preparation, H.Z. and H.K.; writing—review and editing, H.Z., H.K., A.R. and M.D.; visualization, H.Z.; supervision, A.R. and M.D. All authors have read and agreed to the published version of the manuscript.

Funding: This research received no external funding.

Data Availability Statement: The data and code are available upon request.

Conflicts of Interest: The authors declare no conflicts of interest.

References

1. Urcan, D.C.; Bică, D. Integrating and modeling the Vehicle to Grid concept in Micro-Grids. In Proceedings of the 2019 International Conference on ENERGY and ENVIRONMENT (CIEM), Timisoara, Romania, 17–18 October 2019. [\[CrossRef\]](#)
2. Srujan, D.; Thogaru, R.; Mitra, A.; Borghate, V.B. Energy management in grid-assisted BESS integrated solar PV-based smart charging station. In Proceedings of the IECON 2019—45th Annual Conference of the IEEE Industrial Electronics Society, Lisbon, Portugal, 14–17 October 2019. [\[CrossRef\]](#)
3. Rangarajan, S.S.; Raman, R.; Singh, A.; Shiva, C.K.; Kumar, R.; Sadhu, P.K.; Collins, E.R.; Senjyu, T. DC microgrids: A propitious smart grid paradigm for Smart Cities. *Smart Cities* **2023**, *6*, 1690–1718. [\[CrossRef\]](#)
4. Al-Ismail, F.S. DC microgrid planning, operation, and control: A comprehensive review. *IEEE Access* **2021**, *9*, 36154–36172. [\[CrossRef\]](#)
5. Garcia Elvira, D.; Valderrama Blavi, H.; Cid Pastor, A.; Martinez Salamero, L. Efficiency optimization of a variable bus voltage DC microgrid. *Energies* **2018**, *11*, 3090. [\[CrossRef\]](#)
6. Ullah, S.; Haidar, A.M.; Hoole, P.; Zen, H.; Ahfock, T. The current state of Distributed Renewable Generation, challenges of interconnection and opportunities for energy conversion based DC microgrids. *J. Clean. Prod.* **2020**, *273*, 122777. [\[CrossRef\]](#)
7. Dutta, S.; Johnson, B. A Practical Digital Implementation of Completely Decentralized Ripple Minimization in Parallel-Connected DC–DC Converters. *IEEE Trans. Power Electron.* **2022**, *37*, 14422–14433. [\[CrossRef\]](#)
8. Xia, Y.; Wei, W.; Long, T.; Blaabjerg, F.; Wang, P. New analysis framework for transient stability evaluation of DC microgrids. *IEEE Trans. Smart Grid* **2020**, *11*, 2794–2804. [\[CrossRef\]](#)
9. Li, X.; Li, Z.; Guo, L.; Zhu, J.; Wang, Y.; Wang, C. Enhanced dynamic stability control for low-inertia hybrid AC/DC microgrid with distributed energy storage systems. *IEEE Access* **2019**, *7*, 91234–91242. [\[CrossRef\]](#)
10. El-Shahat, A.; Sumaiya, S. DC-microgrid system design, control, and analysis. *Electronics* **2019**, *8*, 124. [\[CrossRef\]](#)
11. Twaisan, K.; Barişçi, N. Integrated Distributed Energy Resources (DER) and Microgrids: Modeling and Optimization of DERs. *Electronics* **2022**, *11*, 2816. [\[CrossRef\]](#)

12. Naderi, E.; Mirzaei, L.; Pourakbari-Kasmaei, M.; Cerna, F.V.; Lehtonen, M. Optimization of active power dispatch considering unified power flow controller: Application of evolutionary algorithms in a fuzzy framework. *Evol. Intell.* **2023**, *1–31*. [[CrossRef](#)]
13. Naderi, E.; Mirzaei, L.; Trimble, J.P.; Cantrell, D.A. Multi-objective optimal power flow incorporating flexible alternating current transmission systems: Application of a wavelet-oriented evolutionary algorithm. *Electr. Power Components Syst.* **2024**, *52*, 766–795. [[CrossRef](#)]
14. Naderi, E.; Azizivahed, A.; Asrari, A. A step toward cleaner energy production: A water saving-based optimization approach for economic dispatch in modern power systems. *Electr. Power Syst. Res.* **2022**, *204*, 107689. [[CrossRef](#)]
15. Keyhani, A. Smart power grids. In *Smart Power Grids 2011*; Springer: Berlin/Heidelberg, Germany, 2011; pp. 1–25.
16. Zolfaghari, A.; Aminian, E.; Saffari, H. Numerical investigation on entropy generation in the dropwise condensation inside an inclined pipe. *Heat Transf.* **2022**, *51*, 551–577. [[CrossRef](#)]
17. Aghajani, G.; Ghadimi, N. Multi-objective energy management in a micro-grid. *Energy Rep.* **2018**, *4*, 218–225. [[CrossRef](#)]
18. Cheng, L.; Yu, T. Game-theoretic approaches applied to transactions in the open and ever-growing electricity markets from the perspective of power demand response: An overview. *IEEE Access* **2019**, *7*, 25727–25762. [[CrossRef](#)]
19. Mengelkamp, E.; Gärtner, J.; Rock, K.; Kessler, S.; Orsini, L.; Weinhardt, C. Designing microgrid energy markets: A case study: The Brooklyn Microgrid. *Appl. Energy* **2018**, *210*, 870–880. [[CrossRef](#)]
20. Xiong, X.; Yang, Y. A photovoltaic-based DC microgrid system: Analysis, design and experimental results. *Electronics* **2020**, *9*, 941. [[CrossRef](#)]
21. Prasad, B.H.; Thogaru, R.B.; Mitra, A. Integration of Electric Vehicles to DC microgrid Enabling V2G and G2V. In Proceedings of the 2022 IEEE Students Conference on Engineering and Systems (SCES), Prayagraj, India, 1–3 July 2022; pp. 1–6. [[CrossRef](#)]
22. Farrokhhabadi, M.; König, S.; Cañizares, C.A.; Bhattacharya, K.; Leibfried, T. Battery energy storage system models for microgrid stability analysis and dynamic simulation. *IEEE Trans. Power Syst.* **2017**, *33*, 2301–2312. [[CrossRef](#)]
23. Banerji, A.; Sharma, K.; Singh, R.R. Integrating Renewable Energy and Electric Vehicle Systems into Power Grid: Benefits and Challenges. In Proceedings of the 2021 Innovations in Power and Advanced Computing Technologies (i-PACT), Kuala Lumpur, Malaysia, 27–29 November 2021; pp. 1–6. [[CrossRef](#)]
24. Zhao, Q.; Xu, J.; Yang, J.; Liao, K.; He, Z. Three-stage optimal control approach of DC microgrid considering EVs interval prediction and BESS rolling power limits. *CSEE J. Power Energy Syst.* **2023**, *1–11*. [[CrossRef](#)]
25. Li, S.; Zhao, P.; Gu, C.; Li, J.; Huo, D.; Cheng, S. Aging mitigation for battery energy storage system in electric vehicles. *IEEE Trans. Smart Grid* **2022**, *14*, 2152–2163. [[CrossRef](#)]
26. Wang, M.H.; Tan, S.C.; Lee, C.K.; Hui, S. A configuration of storage system for DC microgrids. *IEEE Trans. Power Electron.* **2017**, *33*, 3722–3733. [[CrossRef](#)]
27. Fazal, S.; Haque, M.E.; Arif, M.T.; Gargoom, A.; Oo, A.M.T. Grid integration impacts and control strategies for renewable based microgrid. *Sustain. Energy Technol. Assessments* **2023**, *56*, 103069. [[CrossRef](#)]
28. Sepasi, S.; Talichet, C.; Pramanik, A.S. Power Quality in Microgrids: A Critical Review of Fundamentals, Standards, and Case Studies. *IEEE Access* **2023**, *11*, 108493–108531. [[CrossRef](#)]
29. Sevostyanov, N.A.; Gorbunov, R.L. Control Strategy to Mitigate Voltage Ripples in Droop-Controlled DC Microgrids. *IEEE Trans. Power Electron.* **2023**, *38*, 15377–15389. [[CrossRef](#)]
30. Chaturvedi, S.; Fulwani, D.; Patel, D. Dynamic virtual impedance-based second-order ripple regulation in DC microgrids. *IEEE J. Emerg. Sel. Top. Power Electron.* **2021**, *10*, 1075–1083. [[CrossRef](#)]
31. Ferahtia, S.; Djerioui, A.; Rezk, H.; Chouder, A.; Houari, A.; Machmoum, M. Adaptive droop based control strategy for DC microgrid including multiple batteries energy storage systems. *J. Energy Storage* **2022**, *48*, 103983. [[CrossRef](#)]
32. Sekhar, P.; Krishna, U. Voltage ripple mitigation in DC microgrid with constant power loads. *IFAC-PapersOnLine* **2019**, *52*, 300–305. [[CrossRef](#)]
33. Srivastava, C.; Tripathy, M. DC microgrid protection issues and schemes: A critical review. *Renew. Sustain. Energy Rev.* **2021**, *151*, 111546. [[CrossRef](#)]
34. Hannan, M.A.; Faisal, M.; Ker, P.J.; Begum, R.A.; Dong, Z.Y.; Zhang, C. Review of optimal methods and algorithms for sizing energy storage systems to achieve decarbonization in microgrid applications. *Renew. Sustain. Energy Rev.* **2020**, *131*, 110022. [[CrossRef](#)]
35. Smith, R.; Lukowski, J.; Weaver, W. DC microgrid stabilization through fuzzy control of interleaved heterogeneous storage elements. In Proceedings of the 2018 IEEE 19th Workshop on Control and Modeling for Power Electronics (COMPEL), Padua, Italy, 25–28 June 2018. [[CrossRef](#)]
36. Smith, R.; Lukowski, J.; Weaver, W. Fuzzy control of energy storage systems in DC microgrids. In Proceedings of the 2019 IEEE 20th Workshop on Control and Modeling for Power Electronics (COMPEL), Toronto, ON, Canada, 17–20 June 2019. [[CrossRef](#)]
37. Taheri, B.; Shahhoseini, A. Direct current (DC) microgrid control in the presence of electrical vehicle/photovoltaic (EV/PV) systems and hybrid energy storage systems: A Case study of grounding and protection issue. *IET Gener. Transm. Distrib.* **2023**, *17*, 3084–3099. [[CrossRef](#)]
38. Zadeh, L. Outline of a new approach to the analysis of complex systems and decision processes. *IEEE Trans. Syst. Man, Cybern.* **1973**, *1*, 28–44. [[CrossRef](#)]

39. Kennedy, J.; Eberhart, R. Particle swarm optimization. In Proceedings of the ICNN'95—International Conference on Neural Networks, Perth, WA, Australia, 27 November–1 December 1995. [[CrossRef](#)]
40. Karimi, H.; Dashti, R. Comprehensive framework for capacitor placement in distribution networks from the perspective of distribution system management in a restructured environment. *Int. J. Electr. Power Energy Syst.* **2016**, *82*, 11–18. [[CrossRef](#)]

Disclaimer/Publisher's Note: The statements, opinions and data contained in all publications are solely those of the individual author(s) and contributor(s) and not of MDPI and/or the editor(s). MDPI and/or the editor(s) disclaim responsibility for any injury to people or property resulting from any ideas, methods, instructions or products referred to in the content.